Pergamon

Spectrochimica Acta, Vol. 50A, No. 3, pp. 493–507, 1994

0584–8539/94 $6.00 + 0.00

Magnetic circular dichroism spectroscopy of zinc(II) tetraphenylporphyrin–ligand complexes: the effect of the axial ligand on spectral properties

ELISABETH T. KINTNER,*† JOSEPH V. NARDO*‡ and JOHN H. DAWSON*§‖

* Department of Chemistry and Biochemistry and § The School of Medicine, University of South Carolina, Columbia, SC 29208, U.S.A.

(*Received* 28 *April* 1992; *accepted* 4 *May* 1992)

Abstract—The magnetic circular dichroism (MCD) spectra in the UV–visible spectral region (300–700 nm) of an extensive set of zinc tetraphenylporphyrin (ZnTPP) complexes with oxygen, nitrogen and sulfur donor axial ligands are reported. Because zinc porphyrins do not change oxidation or spin states and only bind one axial ligand, this study evaluates the effect of the axial ligand on the MCD spectral properties. The three types of axial ligand complexes can be discriminated by examination of the MCD band positions and intensities for the Soret, beta and alpha transitions of each ZnTPP adduct.

INTRODUCTION

THE HEME prosthetic group is found at the active site of a large number of metalloproteins [1–3]. The elucidation of the active site structure and mechanism of action of such proteins has been the object of extensive research activity. A wide variety of spectroscopic techniques including electronic absorption, electron paramagnetic resonance, nuclear magnetic resonance, IR absorption, resonance Raman, Mössbauer and magnetic circular dichroism (MCD) have been used to establish the coordination structure of iron porphyrin sites in heme proteins. Each of these techniques has inherent advantages and limitations; in the absence of X-ray crystallography, it is usually necessary to employ several of the aforementioned methods in order to ascertain the coordination structure of metalloporphyrins.

MCD spectroscopy has found wide application in the study of heme proteins because of its sensitivity to changes in the spin and oxidation state of the metal and to the nature of the axial ligand to the metal [4–6]. The present study focuses on the latter factor, namely the influence of the axial ligand on the MCD spectrum of a metalloporphyrin. Zinc(II) tetraphenylporphyrin (ZnTPP) is particularly well suited for such a study because it does not undergo changes in oxidation or spin state, will accept only one axial ligand [7–14] and does not possess empty *d*-orbitals that might participate in bonding. The spectral trends observed for ZnTPP–ligand complexes may therefore be directly attributed to the donor properties of the axial ligand. Information about the relative donor properties of common metalloporphyrin axial ligands should facilitate interpretation of spectral trends observed with metalloporphyrins containing metals that do undergo changes in spin and oxidation state.

In an earlier publication, we presented a limited study of the MCD spectra of ZnTPP complexes with oxygen and nitrogen donor axial ligands [15]. We were able to distinguish between oxygen and nitrogen coordination to the zinc based on wavelength shifts and intensity changes in the MCD spectra. The present report extends our previous studies to include a much larger and more comprehensive set of neutral nitrogen and oxygen donor axial ligand complexes. We have also examined adducts with uncharged sulfur donor axial ligands as well as several complexes containing anionic axial ligands.

† Present address: Department of Chemistry, University of Pittsburgh/Johnstown, Johnstown, PA 15904, U.S.A.

‡ Present address: Warner Lambert Laboratories, Morris Plains, NJ 07950, U.S.A.

‖ Author to whom all correspondence should be addressed.

Abbreviations: MCD, magnetic circular dichroism; ZnTPP, zinc(II) tetraphenylporphyrin; ZnPPIXDME, zinc(II) protoporphyrin IX dimethyl ester.

Herein, we evaluate the utility of MCD spectroscopy for axial ligand identification in ZnTPP complexes.

EXPERIMENTAL

Reagents and materials

ZnTPP was prepared as described previously [15], zinc(II) protoporphyrin IX dimethyl ester (ZnPPIXDME) was purchased from Porphyrin Products. Reagent grade benzene was washed with acid and distilled from sodium benzophenone ketyl [16]. Reagent grade dimethylsulfoxide was distilled under vacuum prior to use. All ligands (reagent grade, Aldrich) were recrystallized or distilled before use [15, 16]. Propanethiolate was prepared as previously described [17]. Potassium imidazolate was prepared by the reaction of imidazole with potassium hydride. Potassium superoxide (Alfa) was used as received.

Preparation of samples for spectroscopic analysis

Zinc porphyrin complexes with neutral ligands were generated by the addition of a concentrated solution of the zinc porphyrin in benzene to the neat ligand or to a saturated benzene solution of the solid ligand. Due to high moisture sensitivity, all atomic salts, as well as porphyrin complexes with anionic ligands, were prepared in a Vacuum Atmospheres inert atmosphere box and were handled in sealed cuvettes. Complexes with anionic ligands were prepared by adding a concentrated solution of the zinc porphyrin to a solution of the anionic species (imidazolate, 0.5 M in dimethylsulfoxide; potassium superoxide, 0.15 M solubilized in dimethylsulfoxide with dicyclohexyl-18-crown-6 [19]; potassium propanethiolate, 0.5 M solubilized in benzene with dicyclohexyl-18-crown-6). The MCD spectra of the imidazolate and superoxide complexes were recorded in dimethylsulfoxide; benzene was used as the solvent in all other cases. Porphyrin concentrations did not exceed 4×10^{-5} M. In all cases, absorbances in the visible region (500–700 nm) did not exceed 0.5 in a 1.0 cm cuvette; maximum absorbances of about 1.2 were used to study samples in the Soret region (300–500 nm).

Spectroscopic methods

Electronic absorption spectra were recorded on Varian-Cary 210 or 219 spectrophotometers. MCD spectra were obtained using a JASCO J-40C spectropolarimeter equipped with a 1.5 T electromagnet calibrated with $K_3Fe(CN)_6$ [19]. Electronic absorption spectra were recorded before and after the scan; only when the two exhibited less than 5% difference were the MCD spectra deemed valid. MCD scans have been normalized to path length, concentration and magnetic field strength $[(M \cdot cm \cdot T)^{-1}]$ [20].

The MCD spectra of ZnTPP complexes are dominated by positive (i.e. positive/negative band pattern with increasing wavelength) derivative-shaped features. The MCD spectra of ZnTPP complexes can be compared using five parameters: the PEAK, TROUGH and CROSSOVER wavelengths together with the PEAK–TROUGH intensity difference and the PEAK/TROUGH intensity ratio. The CROSSOVER, PEAK and TROUGH wavelengths are related to peak position whereas the PEAK–TROUGH amplitude and the PEAK/TROUGH ratio are related to the bandshape.

RESULTS AND DISCUSSION

The band, signal intensity and transition energy of MCD spectral features are a function of the electronic structure of the chromophore under investigation [21–23]. MCD transitions can be either positive or negative in amplitude, possess narrow peak widths at half-height and can provide a unique "spectral fingerprint" for a particular metalloporphyrin–ligand complex. In contrast, the more commonly employed technique of electronic absorption spectroscopy produces broader monosignate features with metalloporphyrins that are of less diagnostic utility.

Relative to four-coordinate ZnTPP, the electronic absorption [12] spectra of coordination complexes of ZnTPP are shifted to longer wavelength, with a concomitant increase

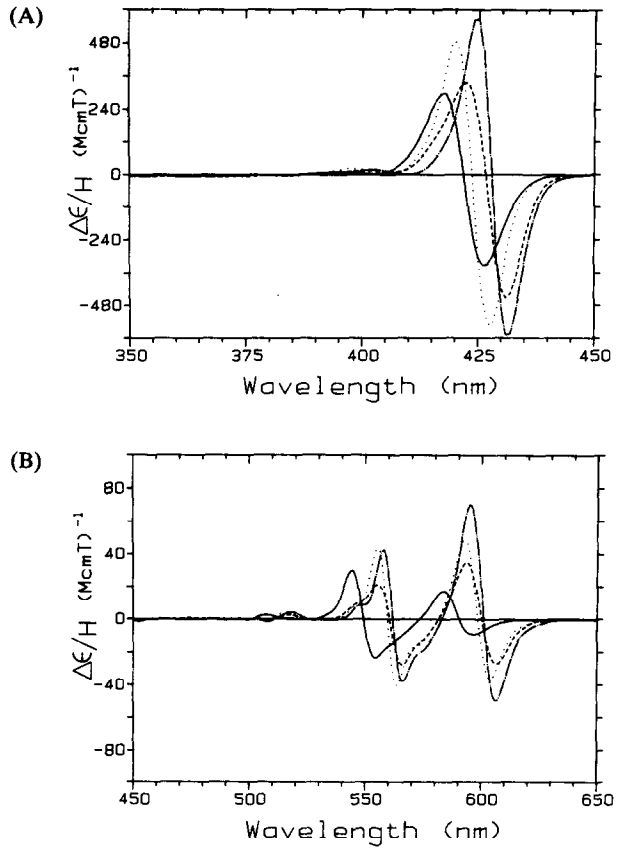

Fig. 1. MCD spectra in the Soret (A) and visible (B) regions for ZnTPP (————) in benzene, and its complexes with n-octylamine (–·–·–), n-butanol (·····), and butanethiol (---------). The ligand adducts were examined using the neat liquid ligand as solvent. Spectra were obtained at 24°C. See the Experimental section for additional details.

in the alpha band intensity relative to that of the beta band ($\varepsilon_\alpha/\varepsilon_\beta$). These spectral changes were attributed to a transfer in electron density from the axial ligand to the porphyrin ring via the zinc atom [12, 24, 25]. The magnitudes of the spectral changes are proportional to the degree of charge transferred from the axial ligand to the porphyrin ring. Thus, the donor properties of the axial ligand will affect the magnitude of the spectral shifts. An axial ligand capable of transferring a large amount of negative charge, such as an anion, will correspondingly produce larger red-shifts and increases in the magnitude of $\varepsilon_\alpha/\varepsilon_\beta$. Because MCD spectra are inherently more distinctive than electronic absorption spectra (see above), we have sought in the present study to examine the ability of the technique to respond to changes in the donor properties of axial ligands in order to see if the spectral changes seen upon axial ligand binding to zinc porphyrins might be more readily observed with MCD spectroscopy.

The present application of MCD spectroscopy is a major extension of an earlier investigation [15] and attempts to establish the utility of MCD to discriminate between neutral and anionic nitrogen, oxygen and sulfur donor complexes of ZnTPP. Because zinc porphyrins do not change oxidation or spin states and only bind one axial ligand, this study directly evaluates the effect of the axial ligand on the MCD spectral properties.

The MCD spectrum of four-coordinate ZnTPP is characterized by positive derivative-shaped bands [25] for the Soret, beta and alpha transitions. Figures 1A and B show the MCD spectra in the Soret and visible regions, respectively, for four-coordinate ZnTPP and its complexes with alkyl-substituted amine nitrogen, alcohol oxygen and thiol sulfur donor axial ligands. The spectra of analogous benzylic-substituted nitrogen, oxygen, and sulfur donor adducts are displayed in Fig. 2A and B. These spectra are representative of the data obtained with a large number of neutral nitrogen, oxygen and sulfur donor axial

ligand adducts of ZnTPP, the MCD parameters of which are listed in Tables 1–3 and summarized in Table 4. The Soret, beta and alpha MCD bands of the ZnTPP axial ligand adducts are red-shifted compared to the corresponding transitions of four-coordinate ZnTPP. The shifts in PEAK, CROSSOVER, and TROUGH wavelengths are most pronounced in the beta and alpha MCD bands. The nitrogen donor-ligated adducts give rise to the greatest wavelength shifts followed by the complexes with sulfur donors and then the oxygen donor-ligated species (Table 4). The Soret and especially the alpha bands for the axial ligand complexes increase in PEAK-TROUGH intensity relative to those of four-coordinate ZnTPP. The intensities of the beta bands increase somewhat relative to that of the four-coordinate species for nitrogen and oxygen donor ligated ZnTPP complexes but actually decrease in intensity for many of the sulfur donor adducts.

Nitrogen donor ligand complexes of ZnTPP

Coordination of a nitrogen donor axial ligand to ZnTPP produces shifts of 6 to 11 nm in the Soret CROSSOVER wavelength (see Table 1). The beta and alpha MCD bands of ZnTPP undergo even larger red-shifts of 16 and 15 nm, respectively, upon complexation by nitrogenous axial ligands. Distinct changes in the band shape as well as position of the MCD spectra of nitrogen donor-ligated species allow easy differentiation from the spectrum of four-coordinate ZnTPP. The PEAK–TROUGH amplitudes of all three bands increase for the nitrogen donor adducts, and the alpha and beta bands become more symmetrical (PEAK/TROUGH closer to 1.0). The alpha and beta bands are much more sensitive to spectral changes upon coordination of an axial ligand [26]. As can be

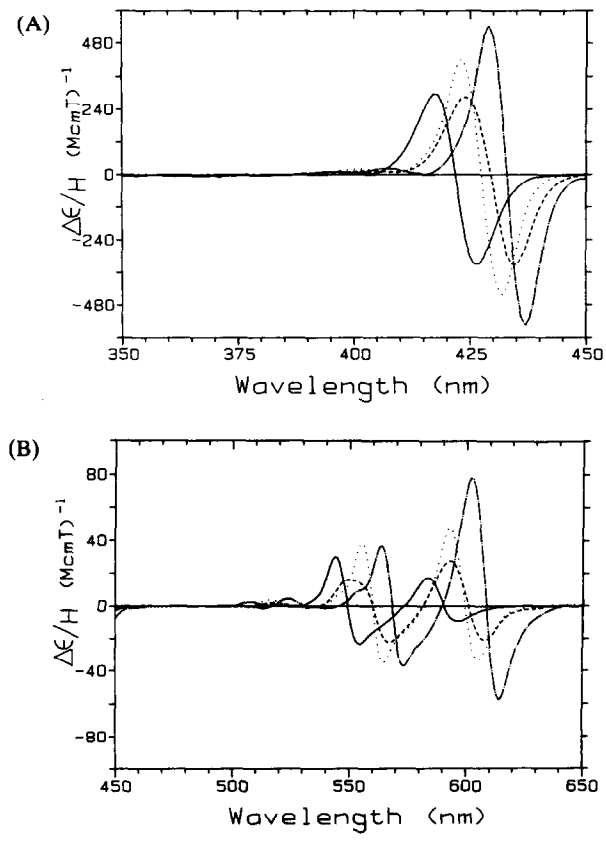

Fig. 2. MCD spectra in the Soret (A) and visible (B) regions for ZnTPP (————) in benzene, and its complexes with benzylamine (–·–·–), benzyl alcohol (·····), and chlorobenzylmercaptan (---------). The ligand adducts were examined using the neat liquid ligand as solvent. Spectra were obtained at 24°C. See the Experimental section for additional details.

Table 1. MCD data for nitrogen donor ligand complexes with ZnTPP

Ligand	Soret*					Beta*					Alpha*				
	PEAK	CROSS-OVER	TROUGH	PEAK–TROUGH	PEAK/TROUGH	PEAK	CROSS-OVER	TROUGH	PEAK–TROUGH	PEAK/TROUGH	PEAK	CROSS-OVER	TROUGH	PEAK–TROUGH	PEAK/TROUGH
No ligand†	417	422	427	624	−0.91	544	549	554	53	−1.30	583	590	597	26.4	−1.81
	(297)		(−327)			(30)		(−23)			(17)		(−9.4)		
Benzylamine‡	429	433	437	1004	−0.98	564	568	573	68	−1.00	602	609	614	123	−1.37
	(496)		(−508)			(34)		(−34)			(71)		(−52)		
n-Octylamine§‖	425	428	431	1156	−0.96	558	562	566	81	−1.13	595	601	606	121	−1.42
	(567)		(−589)			(43)		(−38)			(71)		(−50)		
Pyrrole‡	426	430	435	781	−0.76	562	566	571	49	−0.69	600	606	612	92	−1.19
	(338)		(−443)			(20)		(−29)			(50)		(−42)		
Pyrrolidine‡	427	431	435	1036	−0.97	564	568	573	70	−1.06	603	609	614	122	−1.39
	(509)		(−527)			(36)		(−34)			(71)		(−51)		
4-Methyl morpholine‡	423	427	432	903	−0.86	558	563	568	62	−0.94	592	602	608	93	−1.33
	(417)		(−486)			(30)		(−32)			(53)		(−40)		
Substituted pyridines															
Pyridine‡‖	425	429	432	989	−0.98	559	563	568	68	−1.06	596	603	608	106	−1.41
	(490)		(−499)			(35)		(−33)			(62)		(−44)		
Pyridine§‖	425	428	432	991	−0.99	559	563	568	69	−1.09	596	603	608	97	−1.49
	(492)		(−499)			(36)		(−33)			(58)		(−39)		
2-Picoline‡	425	429	434	814	−0.92	559	564	569	65	−1.03	597	604	609	91	−1.33
	(389)		(−425)			(33)		(−32)			(52)		(−39)		
3-Picoline‡	427	430	434	997	−0.99	561	566	570	67	−1.09	599	606	611	107	−1.43
	(497)		(−500)			(35)		(−32)			(63)		(−44)		
4-Picoline‡	427	430	434	966	−0.94	562	568	570	69	−1.03	599	606	611	110	−1.34
	(469)		(−497)			(35)		(−34)			(63)		(−47)		
3,5-Lutidine‡	426	430	434	963	−0.95	561	565	569	74	−1.06	598	605	610	116	−1.37
	(470)		(−493)			(38)		(−36)			(67)		(−49)		
2,4-Lutidine‡	425	429	433	995	−0.88	559	563	568	74	−1.06	597	603	608	103	−1.34
	(465)		(−530)			(38)		(−36)			(59)		(−44)		
2,6-Lutidine‡	425	430	434	921	−0.92	561	565	569	73	−1.09	598	605	610	108	−1.40
	(442)		(−479)			(38)		(−35)			(63)		(−45)		

(*continued overleaf*)

Table 1—*continued*

Ligand	Soret* PEAK	CROSS-OVER	TROUGH	PEAK–TROUGH	PEAK/TROUGH	Beta* PEAK	CROSS-OVER	TROUGH	PEAK–TROUGH	PEAK/TROUGH	Alpha* PEAK	CROSS-OVER	TROUGH	PEAK–TROUGH	PEAK/TROUGH
Imadazole§‖	427	430	433	921	−0.97	561	565	570	76	−1.05	599	605	611	120	−1.50
	(454)		(−467)			(39)		(−37)			(72)		(−48)		
1-Methyl-	426	429	433	1234	−0.98	561	565	570	75	−1.03	599	605	611	119	−1.48
imadazole‡‖	(610)		(−624)			(38)		(−37)			(71)		(−48)		
1-Methyl-	426	430	433	1138	−1.00	561	566	570	76	−1.11	599	605	611	116	−1.42
imadazole§‖	(569)		(−569)			(40)		(−36)			(68)		(−48)		
2-Methyl-	426	430	433	1020	−0.96	560	564	569	71	−1.09	598	604	609	109	−1.42
imidazole§	(500)		(−520)			(37)		(−34)			(64)		(−45)		
2-Ethyl-	426	429	432	1079	−0.95	559	563	568	75	−1.08	596	602	608	113	−1.46
imidazole§‖	(527)		(−552)			(39)		(−36)			(67)		(−46)		
1-Phenyl-	426	429	433	1150	−1.00	561	565	570	73	−1.03	599	605	611	115	−1.45
imidazole§	(576)		(−574)			(37)		(−36)			(68)		(−47)		
2-Phenyl-	426	429	432	1071	−0.98	561	566	570	72	−1.06	599	603	608	118	−1.41
imidazole§	(530)		(−541)			(37)		(−35)			(69)		(−49)		
4-Phenyl-	426	429	433	1072	−0.96	561	564	570	70	−1.06	599	605	611	113	−1.46
imidazole§	(526)		(−546)			(36)		(−34)			(67)		(−46)		
4,5-Diphenyl-	426	429	432	1041	−0.96	560	565	8570	70	−1.06	599	605	611	107	−1.33
imidazole§	(510)		(−531)			(36)		(−34)			(61)		(−46)		
2,4,5-Triphenyl-								Not formed							
imidazole¶															

* The PEAK, CROSSOVER and TROUGH wavelengths are given in nanometers. The MCD PEAK–TROUGH intensities are given in parentheses as $\Delta\varepsilon/H$, molar magnetic absorptivity $(M \cdot cm \cdot T)^{-1}$. Spectra were measured at 24°C.

† Ligand-free ZnTPP in benzene.

‡ Spectrum obtained using the neat ligand as solvent.

§ Spectrum obtained as the 99% saturated complex in benzene.

‖ Spectrum previously recorded; see Ref. [15].

¶ No spectral change observed in saturated solution.

Table 2. MCD data for nitrogen donor ligand complexes with ZnTPP

	Soret*					Beta*					Alpha*				
Ligand	PEAK	CROSS-OVER	TROUGH	PEAK–TROUGH	PEAK/TROUGH	PEAK	CROSS-OVER	TROUGH	PEAK–TROUGH	PEAK/TROUGH	PEAK	CROSS-OVER	TROUGH	PEAK–TROUGH	PEAK/TROUGH
No ligand†	417	422	427	624	−0.91	544	549	554	53	−1.30	583	590	597	26.4	−1.81
	(297)		(−327)			(30)		(−23)			(17)		(−9.4)		
Ethanol‡§	418	421	424	1091	−0.92	552	556	560	78	−1.11	589	595	600	79	−1.39
	(523)		(−568)			(41)		(−37)			(46)		(−33)		
Ethanol‡‖	420	424	428	783	−0.96	552	556	561	65	−1.24	590	596	601	62	−1.48
	(384)		(−399)			(36)		(−29)			(37)		(−25)		
n-Butanol§	420	424	428	952	−0.89	555	560	564	77	−1.08	593	598	604	78	−1.36
	(447)		(−505)			(40)		(−37)			(45)		(−33)		
iso-Butanol§	419	422	425	1136	−0.93	552	556	560	78	−1.11	589	595	600	77	−1.40
	(548)		(−588)			(41)		(−37)			(45)		(−32)		
sec-Butanol§	419	422	426	1088	−0.94	553	557	562	78	−1.11	591	596	602	76	−1.38
	(526)		(−562)			(41)		(−37)			(44)		(−32)		
tert-Butanol§			Not recorded			549	554	558	62	−1.00	587	593	598	57	−1.38
						(31)		(−31)			(33)		(−24)		
Benzyl alcohol§	423	427	432	792	−0.95	555	560	565	67	−1.09	593	599	605	75	−1.42
	(386)		(−406)			(35)		(−32)			(44)		(−31)		
1,4-Dioxane§	419	423	427	923	−0.90	553	558	562	64	−1.11	591	597	603	73	−1.43
	(437)		(−486)			(34)		(−30)			(43)		(−30)		
Tetrahydrofuran‡§	418	421	425	1036	−0.99	550	554	558	74	−1.18	587	593	599	71	−1.45
	(515)		(−521)			(40)		(−34)			(42)		(−29)		
Tetrahydroifuran‡‖	420	423	427	947	−0.96	550	555	559	73	−1.15	588	594	599	68	−1.50
	(464)		(−483)			(39)		(−34)			(41)		(−27)		
Dimethyl sulfoxide‡§			Not recorded			558	562	567	77	−1.08	595	602	607	109	−1.32
						(40)		(−37)			(62)		(−47)		
Dimethyl sulfoxide‡‖	423	426	430	1042	−0.98	555	559	563	77	−1.08	592	598	604	86	−1.45
	(516)		(−526)			(40)		(−37)			(51)		(−35)		
Dimethyl formamide‡§			Not recorded			554	559	563	72	−1.12	590	596	602	91	−1.46
						(38)		(−34)			(54)		(−37)		
No ligand†	417	422	427	624	−0.91	544	549	554	53	−1.30	583	590	597	26.4	−1.81
	(297)		(−327)			(30)		(−23)			(17)		(−9.4)		

(*continued overleaf*)

Table 2—*continued*

	Soret*					Beta*					Alpha*				
Ligand	PEAK	CROSS-OVER	TROUGH	PEAK–TROUGH	PEAK/TROUGH	PEAK	CROSS-OVER	TROUGH	PEAK–TROUGH	PEAK/TROUGH	PEAK	CROSS-OVER	TROUGH	PEAK–TROUGH	PEAK/TROUGH
Dimethyl formamide‡‖	422 (502)	425	429 (−513)	1015	−0.98	553 (37)	557	562 (−33)	70	−1.12	592 (50)	598	604 (−34)	84	−1.47
Cyclohexanone§	420 (448)	424	428 (−495)	943	−0.91	553 (36)	558	562 (−32)	68	−1.13	591 (37)	597	603 (−26)	63	−1.42
Methyl ethyl ketone§	418 (417)	422	425 (−449)	866	−0.93	552 (31)	557	561 (−29)	60	−1.07	590 (33)	596	602 (−25)	58	−1.32
Benzaldehyde§	423 (291)	428	433 (−315)	606	−0.92	552 (30)	559	565 (−26)	46	1.15	592 (32)	598	605 (−23)	55	−1.39
4-Butyrolactone§	419 (338)	423	429 (−389)	727	−0.87	554 (33)	558	563 (−30)	63	−1.10	591 (41)	597	603 (−28)	69	−1.54
Ethyl acetate§	416 (382)	420	424 (−471)	853	−0.81	551 (32)	555	560 (−31)	63	−1.03	589 (34)	594	600 (−25.0)	59.0	−1.36
Acetic acid¶								Not formed							

* The PEAK, CROSSOVER and TROUGH wavelengths are given in nanometers. The MCD PEAK–TROUGH intensities are given in parentheses as $\Delta\varepsilon/H$, molar magnetic absorptivity $(M \cdot cm \cdot T)^{-1}$. Spectra were measured at 24°C.

† Ligand-free ZnTPP in benzene.

‡ Spectrum previously recorded; see Ref. [15].

§ Spectrum obtained using the neat ligand as solvent.

‖ Spectrum obtained as the 99% saturated complex in benzene.

¶ Species demetallates to form the dication of ZnTPP.

Table 3. MCD data for sulfur donor ligand complexes with ZnTPP

Ligand	Soret*					Beta*					Alpha*				
	PEAK	CROSS-OVER	TROUGH	PEAK–TROUGH	PEAK/TROUGH	PEAK	CROSS-OVER	TROUGH	PEAK–TROUGH	PEAK/TROUGH	PEAK	CROSS-OVER	TROUGH	PEAK–TROUGH	PEAK/TROUGH
No ligand†	417 (297)	422	427 (−327)	624	−0.91	544 (30)	549	554 (−23)	53	−1.30	583 (17)	590	597 (−9.4)	26.4	−1.81
Benzyl mercaptan‡			Not formed					Not formed					Not formed		
Chlorobenzyl-mercaptan§	424 (262)	429	435 (−304)	566	−0.86	550 (15)	560	567 (−20)	35	−0.75	593 (25)	601	608 (−19)	44	−1.32
Thiophenol‡			Not formed					Not formed					Not formed		
Methyl sulfide§	424 (383)	429	434 (−461)	844	−0.83	554 (24)	560	567 (−27)	51	−0.89	593 (36)	601	608 (−27)	63	−1.36
1,4-Thioxane§	422 (385)	427	432 (−345)	730	−1.12	553 (31)	559	564 (−23)	54	−1.35	592 (40)	599	605 (−23)	63	−1.74
2-Mercaptoethanol§	423 (397)	427	432 (−440)	837	−0.90	556 (35)	561	565 (−31)	66	−1.13	594 (45)	600	606 (−32)	77	−1.40
Butanethiol§	422 (309)	427	431 (−414)	723	−0.75	556 (20)	560	566 (−25)	45	−0.77	593 (32)	600	606 (−24)	56	−1.33
Octanethol§	423 (273)	427	431 (−383)	656	−0.71	556 (19)	560	566 (−24)	43	−0.79	594 (31)	600	606 (−23)	54	−1.35
Thiphene§	419 (258)	425	431 (−283)	541	−0.91	546 (22)	553	565 (−17)	39	−1.29	588 (15)	598	606 (−11)	26	−1.36
Tetrahydro-thiophene§	427 (394)	431	436 (−394)	788	−1.00	559 (27)	564	569 (−25)	52	−1.08	598 (47)	605	611 (−30)	77	−1.57

* The PEAK, CROSSOVER and TROUGH wavelengths are given in nanometers. The MCD PEAK–TROUGH intensities are given in parentheses as $\Delta\varepsilon/H$, molar magnetic absorptivity $(M \cdot cm \cdot T)^{-1}$. Spectra were measured at 24°C.

† Ligand-free ZnTPP in benzene.

‡ Species demetallates to form the dication of ZnTPP.

§ Spectrum obtained using the neat ligand as solvent.

seen in Table 1, the CROSSOVER is shifted 11–19 nm to the red for both bands and the amplitude of the alpha band increases dramatically (three- to four-fold).

The MCD spectra of a series of ZnTPP–nitrogen donor ligand complexes prepared using sterically hindered pyridines and imidazoles were examined to determine whether steric influences within a ligand class would give rise to discernable spectral changes. As can be seen in Table 1, neither complexes with substituted pyridines nor imidazoles display appreciable spectral differences from the parent adducts with unsubstituted pyridine and imidazole. Of course, sufficient steric bulk can prevent complex formation, as in the case of 2,4,5-triphenylimidazole (Table 1).

Oxygen donor ligand complexes of ZnTPP

Table 2 shows the MCD spectral data for oxygen donor axial ligand complexes of ZnTPP. The CROSSOVER wavelength of the Soret MCD band of ZnTPP red-shifts by 6 nm or less upon binding of oxygen donor axial ligands. Red-shifts in the beta and alpha bands average 8 and 6 nm, respectively. These shifts are considerably smaller than those seen with nitrogenous axial ligands. As with the ZnTPP adducts with nitrogenous axial ligands, the PEAK–TROUGH amplitudes of all three bands increase and the beta and alpha derivative-shaped MCD bands become more symmetrical upon coordination of oxygen donor axial ligands to ZnTPP. The PEAK–TROUGH intensity increase is most pronounced in the alpha band of oxygen donor ligated ZnTPP, which have three-fold higher intensities on the average.

Table 2 includes data for several adducts prepared using the neat oxygen donor ligand as solvent and as the 99% saturated complex in benzene. Very little difference is seen between the spectra of the species in benzene and in the neat ligand.

Table 4. Summary of MCD data for ligand complexes of ZnTPP*

Ligand type	PEAK	CROSS-OVER	TROUGH	PEAK–TROUGH
Soret				
No ligand	417	422	427	624
N donor	435.9 ± 1.2	429.5 ± 1.2	433.2 ± 1.3	1011 ± 108
O donor	420.4 ± 2.8	424.4 ± 2.2	427.5 ± 2.7	925 ± 146
S donor	423.0 ± 2.3	427.8 ± 1.8	432.8 ± 2.0	710 ± 115
Beta				
No ligand	544	549	554	53
N donor	560.5 ± 1.6	564.4 ± 2.1	569.5 ± 1.6	70 ± 6
O donor	552.8 ± 2.1	557.4 ± 2.2	561.8 ± 2.4	69 ± 8
S donor	553.8 ± 4.1	559.6 ± 3.1	566.1 ± 1.5	48 ± 10
Alpha				
No ligand	583	590	597	26.4
N donor	598.1 ± 2.3	604.6 ± 2.0	610.0 ± 2.0	110 ± 10
O donor	590.5 ± 2.1	596.4 ± 2.2	602.2 ± 2.4	73 ± 13
S donor	593.1 ± 2.7	600.5 ± 2.1	607.0 ± 1.9	58 ± 17
Alpha (PEAK–TROUGH)/beta (PEAK–TROUGH)				
No ligand		0.50		
N donor		1.57		
O donor		1.06		
S donor		1.21		

* Based on data presented in Tables 1–3. The PEAK, CROSSOVER and TROUGH wavelengths are given in nanometers. The MCD PEAK–TROUGH intensities are given as $\Delta\varepsilon/H$, molar magnetic absorptivity $(M \cdot cm \cdot T)^{-1}$.

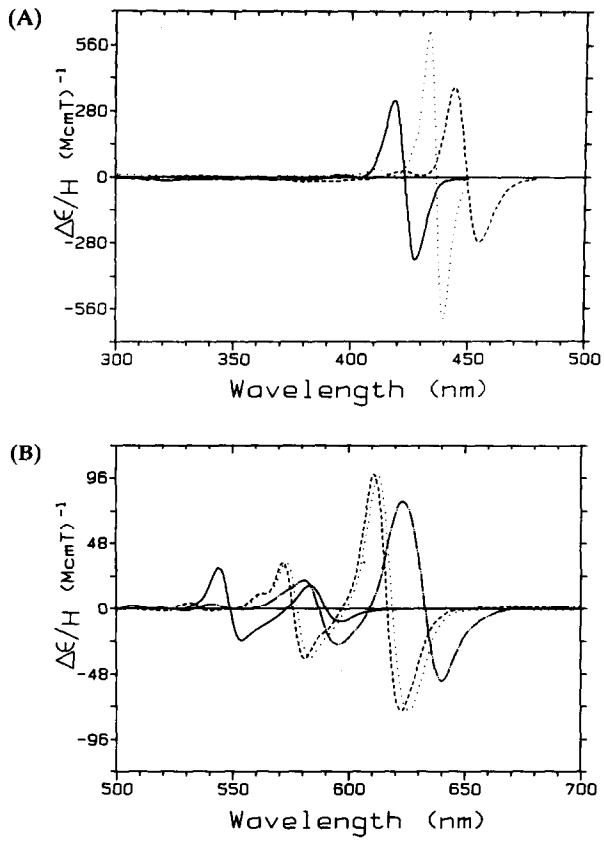

Fig. 3. MCD spectra; in the Soret (A) and visible (B) regions for ZnTPP (————) and its complexes with imidazolate (A, ····· ; B, ---------), propanethiolate (A, --------- ; B, –·–·–) and superoxide (A, not measured; B, ·····). Spectra were obtained at 24°C in benzene. See the Experimental section for additional details.

Sulfur donor ligand complexes of ZnTPP

Table 3 presents the MCD spectral data for sulfur donor ZnTPP axial ligand adducts. The magnitude of the red-shift in the Soret, beta and alpha PEAK, TROUGH, and CROSSOVER wavelengths of these species is intermediate between those of the oxygen and nitrogen donor complexes (Table 4). The changes in PEAK–TROUGH amplitudes for the MCD bands of the sulfur donor-ligated ZnTPP derivatives are consistently the smallest amount of the three types of axial ligand adducts under consideration. The intensities are somewhat higher (~15%) than those of four-coordinate ZnTPP for the Soret transition, slightly lower (~10%) for the beta band, while the alpha transitions are approximately twice as intense. As with the nitrogen and oxygen donor adducts, the alpha and beta MCD bands for the sulfur donor axial ligand complexes are more symmetrical than those of four-coordinate ZnTPP.

ZnTPP *complexes with anionic ligands*

The most dramatic spectral changes among the ZnTPP axial ligand complexes reported herein are seen with adducts involving anionic axial ligands (Fig. 3, Table 5). As noted above, the increased intensities and greater spectral shifts seen with such complexes are due to electronic effects which arise from the transfer of negative charge from anionic axial ligands to the porphyrin ring [12]. Dramatic red-shifts in PEAK, CROSSOVER and TROUGH wavelengths for the Soret, beta and alpha bands and significantly increased PEAK–TROUGH intensities for the alpha transition are observed for the anionic axial ligand complexes of ZnTPP relative to the corresponding ZnTPP adducts with neutral axial ligands and to four-coordinate ZnTPP. For example,

the alpha and beta MCD bands of ZnTPP·imidazolate are significantly more red-shifted from those of ZnTPP than in complexes with neutral imidazoles (26–28 nm vs 12–17 nm). The PEAK–TROUGH intensity of the alpha band of ZnTPP·superoxide is more than $2\frac{1}{2}$ times larger than in complexes with neutral oxygen donors. It is interesting to note that ZnTPP·imidazolate and ZnTPP·superoxide display remarkably similar spectral features in the visible region (Fig. 3). ZnTPP·superoxide was not examined by MCD spectroscopy in the Soret region. As with the other ZnTPP complexes with anionic axial ligands, the derivative-shaped alpha band in the spectrum of ZnTPP·propanethiolate is more than twice as intense as that of the ZnTPP adduct with a neutral sulfur donor such as butanethiol.

The MCD features in the Soret region of the spectrum of ZnTPP·propanethiolate are red-shifted more than any other complex described herein. The likely origin of this exceptionally large red-shift, as suggested by NAPPA and VALENTINE [12], involves an orbital mixing mechanism first proposed by HANSON *et al.* [27] in which a charge transfer absorption from the lone pair p† orbital on the thiolate ligand to the porphyrin π^* orbitals mixes with and splits the doubly degenerate π–π^* Soret band to yield the characteristic "split" Soret spectrum featuring an unusually red-shifted Soret band near 450 nm and an additional peak in the near-UV. HANSON *et al.* proposed this mechanism to explain the unusually red-shifted Soret electronic absorption band of ferrous–CO cytochrome P-450. We have previously reported the use of MCD spectroscopy to examine ZnPPIXDME·propanethiolate [28].

Table 5. MCD data for anion ligand complexes with ZnTPP

Ligand	PEAK	CROSS-OVER	TROUGH	PEAK–TROUGH	PEAK/TROUGH
Soret*					
No ligand	417	422	427	624	−0.91
	(297)		(−327)		
Potassium imidazolate‡	433	436	440	1232	−1.04
	(627)		(−605)		
Potassium superoxide‡§	Not recorded				
Propanethiolate‖¶	444	449	455	661	−1.37
	(382)		(−279)		
Beta*					
No ligand†	544	549	554	53	−1.30
	(30)		(−23)		
Potassium imidazolate‡	572	576	581	71	−0.92
	(34)		(−37)		
Potassium	573	578	583	70	−0.94
superoxide‡§	(34)		(−36)		
Propanethiolate‖¶	581	587	595	47	−0.81
	(21)		(−26)		
Alpha*					
No ligand†	583	590	597	26.4	−1.81
	(17)		(−9.4)		
Potassium imidazolate‡	611	617	623	174	−1.32
	(99)		(−75)		
Potassium	613	619	626	173	−1.31
superoxide‡§	(98)		(−75)		
Propanethiolate‖¶	623	633	640	132	−1.49
	(79)		(−53)		

* The PEAK, CROSSOVER and TROUGH wavelengths are given in nanometers. The MCD PEAK–TROUGH intensities are given in parentheses as $\Delta\varepsilon/H$, molar magnetic absorptivity $(M \cdot cm \cdot T)^{-1}$. Spectra were measured at 24°C.

† Ligand-free ZnTPP in benzene.

‡ Spectrum recorded in DMSO.

§ Anion solubilized as a 0.15 M solution with dicyclohexyl 18-C-6 in DMSO.

‖ Anion solubilized as the potassium salt using dicyclohexyl 18-C-6 in benzene.

¶ Spectrum recorded in benzene.

Sensitivity of MCD spectrum to electronic influences

The MCD spectral changes observed for ZnTPP adducts with neutral and anionic nitrogen, oxygen and sulfur axial ligands parallel trends in their electronic absorption spectra reported by NAPPA and VALENTINE [12]. For example, just as $\varepsilon_\alpha/\varepsilon_\beta$ was shown to increase in parallel with the red-shift of absorption peak wavelengths for ZnTPP complexes [13], the ratio of the alpha MCD band PEAK–TROUGH amplitude to that of the beta band increases as the magnitude of the red-shift in the CROSSOVER wavelengths increases (Table 4). The size of the observed shifts in electronic absorption spectral parameters was shown to depend on the charge and polarizability of the axial ligand [12]. This same reasoning can be applied to explain the patterns observed in the MCD spectra of the species examined herein.

The MCD spectra of ZnTPP adducts with neutral nitrogen, oxygen and sulfur donor axial ligands can be distinguished based on a combination of the magnitudes of the red-shift of the Soret, beta and alpha bands and of their PEAK–TROUGH amplitudes (Table 4). The wavelengths of the PEAKS, CROSSOVERS and TROUGHS of the Soret, beta and alpha bands consistently show the largest average red-shift for the ZnTPP complexes with neutral nitrogenous axial ligands. The spectral features of the adducts with neutral oxygen donor axial ligands are always the least red-shifted, while the spectra of those with neutral sulfur donor axial ligands red-shift by an intermediate amount in all cases (Table 4). However, the wavelengths and signal amplitudes of the Soret MCD band features do not differ enough among the three classes of ligand complexes to be diagnostically useful. In the beta and alpha bands, on the other hand, the magnitudes of the red-shift for the complexes with nitrogen donor axial ligands are sufficiently larger than those of the other two classes of ligand adducts to be of predictive value. The PEAK–TROUGH amplitude in the alpha band is also sufficiently larger for the complexes with nitrogenous axial ligands to be useful in predicting whether a neutral nitrogen donor axial ligand is bound to ZnTPP. The average wavelength values in the beta and alpha bands for the ZnTPP adducts with oxygen and sulfur donor axial ligands do not differ enough to enable the two classes of ligand complexes to be distinguished. Distinction between those two classes can be achieved by examining the PEAK–TROUGH amplitudes of the beta band, where the amplitudes for the ones with sulfur donor axial ligands are significantly smaller than those of the other two classes (Table 4).

Thus, it should be possible to predict whether a ZnTPP-ligand complex has a neutral nitrogen donor axial ligand based on the distinctive wavelength range for the beta and alpha bands and the beta PEAK–TROUGH intensity. Adducts with neutral oxygen or sulfur donor axial ligands should have spectral features in characteristic (although overlapping) wavelength ranges (Table 4) and can be further distinguished based on the PEAK–TROUGH amplitude of the alpha MCD transition. ZnTPP complexes with anionic axial ligands display even more red-shifted spectral features. An insufficient number of such species have been examined to determine how sensitive their spectra are to the exact nature of the axial ligand, although it has already been noted that the MCD spectra of the imidazolate and superoxide adducts are very similar in the beta and alpha bands. The spectrum of the latter was not investigated in the Soret region.

Influence of the porphyrin ligand

The MCD spectra of a few ligand complexes of zinc protoporphyrin IX dimethylester, ZnPPIXDME, have also been examined [28] and the spectral parameters are collected in Table 6. As with ZnTPP–ligand adducts, characteristic changes occur in the MCD spectra upon ligand addition to ZnPPIXDME. The binding of 1-methylimidazole and dimethyl sulfoxide to ZnPPIXDME, for example, leads to red-shifts (13 and 8 nm, respectively) in the Soret CROSSOVER wavelength and to a two-fold increase in PEAK–TROUGH intensity relative to the spectrum of four-coordinate ZnPPIXDME. The spectrum of ZnPPIXDME · propanethiolate exhibits a red-shift of 38 nm in the Soret

Table 6. MCD data for ligand complexes of ZnPPIXDME

Ligand	PEAK	CROSS-OVER	TROUGH	PEAK–TROUGH	PEAK/TROUGH
Soret*					
No ligand†	407	415	423	67	−0.76
	(29)		(−38)		
Dimethylsulfoxide‡	416	423	29	111	−0.79
	(49)		(−62)		
1-Methylimidazole§	421	428	433	149	−0.89
	(70)		(−79)		
Propanethiolate‖	444	453	461	201	−1.28
	(113)		(−88)		
Beta*					
No ligand†	530	538	546	28	−1.00
	(14)		(−14)		
Dimethylsulfoxide‡	538	548	558	34	−0.79
	(15)		(−19)		
1-Methylimidazole§	544	553	563	36	−0.64
	(14)		(−22)		
Propanethiolate‖	565	573	582	52	−0.79
	(23)		(−29)		
Alpha*					
No ligand†	574	579	585	160	−0.98
	(79)		(−81)		
Dimethylsulfoxide‡	581	586	591	145	−0.86
	(67)		(−78)		
1-Methylimidazole§	586	591	596	122	−0.97
	(60)		(−62)		
Propanethiolate‖	598	606	614	34	−0.42
	(10)		(−24)		

* The PEAK, CROSSOVER and TROUGH wavelengths are given in nanometers. The MCD PEAK–TROUGH intensities are given in parentheses as $\Delta\varepsilon/H$, molar magnetic absorptivity $(M \cdot cm \cdot T)^{-1}$. Spectra were measured at 24°C. Porphyrin concentrations did not exceed 4×10^{-5} M.

† Ligand-free ZnPPIXDME in benzene.

‡ Spectrum recorded in neat DMSO.

§ Spectrum recorded in neat 1-methylimidazole

‖ Solubilized as the potassium salt using dicyclohexyl 18-C-6 in benzene.

band and a three-fold amplitude increase. In contrast, the Soret band of ZnTPP·propanethiolate is red-shifted by 27 nm with little change in intensity. The changes exhibited in the beta band (shifts to longer wavelength and modest intensity increases) of ZnPPIXDME on coordination of ligands are similar to those observed for the analogous ZnTPP species.

The PEAK–TROUGH amplitude of the alpha band is most sensitive to the nature of the porphyrin ligand. This is consistent with the results of NAPPA and VALENTINE [12] using electronic absorption spectroscopy. They observed that the magnitude of $\varepsilon_\alpha/\varepsilon_\beta$ *decreases* with increasing red-shift of the peak wavelengths (just the opposite correlation to that seen for ZnTPP adducts; see above). Whereas the MCD alpha band PEAK–TROUGH amplitude increases two- to five-fold on axial ligand coordination to ZnTPP, the opposite occurs for ZnPPIXDME. This difference is most prominent for the thiolate complexes. Relative to four-coordinate ZnTPP, the alpha band of ZnTPP·propanethiolate is five times more intense. By contrast, the alpha band of ZnPPIXDME·propanethiolate is almost five times *less* intense than that of the four-coordinate species. The influence of the porphyrin ligand and peripheral substituents on the porphyrin (electron withdrawing or donating) has been noted to affect the electronic absorption spectra of unsymmetrically substituted derivatives of ZnTPP [29, 30] and metal derivatives of octabromotetraphenylporphyrin [31], the spin state of ferric porphyrins [32] and the MCD spectra of ferrous [33] and ferric porphyrins [34].

Concluding remarks

In this study, we have attempted to evaluate the utility of MCD spectroscopy in the identification of neutral and anionic nitrogen, oxygen, and sulfur donor axial ligands to zinc tetraphenylporphyrin. Two distinct types of changes in the Soret, beta and alpha MCD bands occur upon ligand binding that can be used to this end: red-shifts in the PEAK, CROSSOVER and TROUGH wavelengths and increases in PEAK–TROUGH intensities relative to the those of four-coordinate ZnTPP. ZnTPP complexes with neutral nitrogen, oxygen and sulfur donor axial ligands can be distinguished based on analysis of the red-shifts in band positions and intensity changes. The most dramatic spectral changes are observed for the ZnTPP complexes with anionic ligands.

Acknowledgements—This work was supported by a grant from the National Institutes of Health (GM-26730). The electromagnet for the circular dichroism spectrometer was purchased through a grant from the Research Corporation. We thank Dr. Masanori Sono for helpful suggestions.

References

[1] K. M. Smith (Ed.), *Porphyrins and Metalloporphyrins*. Elsevier, Amsterdam (1975).
[2] D. Dolphin (Ed.), *The Porphyrins*. Academic Press, New York (1979).
[3] A. B. P. Lever and H. B. Gray (Eds), *Iron Porphyrins*, Parts I and II. Addison-Wesley, Reading, MA (1983).
[4] J. H. Dawson and D. M. Dooley, in *Iron Porphyrins*, Part III (Edited by A. B. P. Lever and H. B. Gray), pp. 1, 93. VCH Publishers, New York (1989).
[5] D. M. Dooley and J. H. Dawson, *Coord. Chem. Rev.* **60**, 1 (1984).
[6] B. Holmquist, in *The Porphyrins*, Vol. III (Edited by D. Dolphin), p. 249. Academic Press, New York (1978).
[7] C. H. Kirksey, P. Hambright and C. B. Storm, *Inorg. Chem.* **8**, 2141 (1969).
[8] G. C. Vogel and L. A. Searby, *Inorg. Chem.* **12**, 936 (1973).
[9] G. C. Vogel and J. R. Stahlbush, *Inorg. Chem.* **16**, 950 (1977).
[10] K. M. Kadish and L. R. Shiue, *Inorg. Chem.* **21**, 3623 (1982).
[11] W. A. Kaplan, R. A. Scott and K. S. Suslick, *J. Am. Chem. Soc.* **112**, 1283 (1990).
[12] M. Nappa and J. S. Valentine, *J. Am. Chem. Soc.* **100**, 5075 (1978).
[13] J. V. Nardo and J. H. Dawson, *Inorg. Chim. Acta* **123**, 9 (1986).
[14] In only one case has six-coordination been observed in zinc porphyrins, bis(tetrahydrofuran)ZnTPP. C. K. Schauer, O. P. Anderson, S. S. Eaton and G. R. Eaton, *Inorg. Chem.* **24**, 4082 (1985).
[15] J. V. Nardo and J. H. Dawson, *Spectrosc. Int. J.* **2**, 236 (1983).
[16] D. D. Perrin, W. L. F. Armerego and D. R. Perrin, *Purification of Laboratory Chemicals*, 2nd edn. Pergamon Press, Oxford (1980).
[17] C. K. Chang and D. Dolphin, *Proc. Natn. Acad. Sci. U.S.A.* **73**, 3338 (1976).
[18] J. S. Valentine and A. B. Curtis, *J. Am. Chem. Soc.* **97**, 224 (1975).
[19] J. C. Sutherland, L. E. Vickery and M. P. Klein, *Rev. Sci. Instrum.* **45**, 1089 (1974).
[20] B. Holmquist and B. L. Vallee, *Meth. Enzymol.* **49**, 156 (1978).
[21] A. Ceulemans, W. Oldendorf, C. Görller-Walrand and L. G. Vanquickenbone, *J. Am. Chem. Soc.* **108**, 1155 (1986).
[22] P. J. Stephens, *Ann. Rev. Phys. Chem.* **25**, 210 (1974).
[23] P. J. Stephens, W. Suetaka and P. N. Schatz, *J. Chem. Phys.* **44**, 4592 (1966).
[24] M. Gouterman, F. P. Schwarz, P. D. Smith and D. Dolphin, *J. Chem. Phys.* **59**, 676 (1973).
[25] A. J. McHugh, M. Gouterman and C. Weiss, Jr, *Theor. Chim. Acta* **24**, 346 (1973).
[26] P. J. Spellane, M. Gouterman, A. Antipas, S. Kim and Y. C. Liu, *Inorg. Chem.* **19**, 86 (1980).
[27] L. K. Hanson, W. A. Eaton, S. G. Sligar, I. C. Gunsalus, M. Gouterman and C. R. Connell, *J. Am. Chem. Soc.* **98**, 2672 (1976).
[28] J. V. Nardo, M. Sono and J. H. Dawson, *Inorg. Chim. Acta* **151**, 173 (1988).
[29] G. A. McDermot and F. A. Walker, *Inorg. Chim. Acta* **91**, 95 (1984).
[30] P. Bhyrappa and V. Krishnan, *Inorg. Chem.* **30**, 239 (1991).
[31] D. K. Geiger and W. R. Scheidt, *Inorg. Chem.* **23**, 1970 (1984).
[32] G. E. Toney, L. W. terHaar, J. E. Savrin, A. Gold, W. E. Hatfield and R. Sangaich, *Inorg. Chem.* **23**, 2563 (1984).
[33] E W. Svastits and J. H. Dawson, *Inorg. Chim. Acta* **123**, 83 (1986).
[34] T. Yoshimura, H. Toi, S. Inaba and H. Ogoshi, *Inorg. Chem.* **30**, 4315 (1991).